

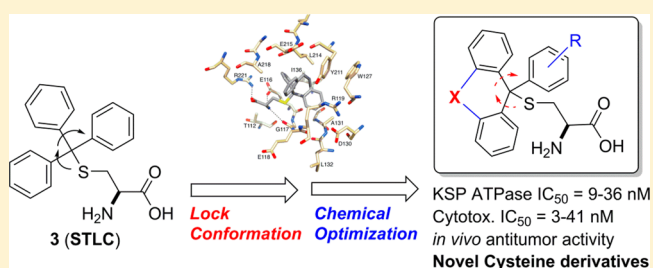
## Structure-Guided Design of Novel L-Cysteine Derivatives as Potent KSP Inhibitors

Naohisa Ogo,<sup>†</sup> Yoshinobu Ishikawa,<sup>‡</sup> Jun-ichi Sawada,<sup>†</sup> Kenji Matsuno,<sup>†,||</sup> Akihiro Hashimoto,<sup>§</sup> and Akira Asai<sup>\*,†</sup><sup>†</sup>Center for Drug Discovery, Graduate School of Pharmaceutical Sciences, University of Shizuoka, Shizuoka 422-8526, Japan<sup>‡</sup>Department of Physical Biochemistry, School of Pharmaceutical Sciences, University of Shizuoka, Shizuoka 422-8526, Japan<sup>§</sup>Tsukuba Research Center, Taiho Pharmaceutical Co., Ltd., 3 Okubo, Tsukuba, Ibaraki 300-2611, Japan

## Supporting Information

**ABSTRACT:** Kinesin spindle protein (KSP), known as Hs Eg5, a member of the kinesin-5 family, plays an important role in the formation and maintenance of the bipolar spindle. We previously reported S-trityl-L-cysteine derivatives as selective KSP inhibitors. Here, we report further optimizations using docking modeling in the LS allosteric binding site, which led to the discovery of several high affinity derivatives with two fused phenyl rings in the trityl group giving low nanomolar range KSP ATPase inhibition. The representative derivatives potently inhibited cell growth of HCT116 cells in correlation with KSP inhibitory activities and significantly suppressed tumor growth in the xenograft model in vivo.

**KEYWORDS:** Kinesin spindle protein, L-cysteine derivative, molecular modeling, differential scanning fluorimetry, HCT-116 xenograft model



Antimitotic agents such as microtubule stabilizers (e.g., taxanes) and destabilizers (e.g., vinca alkaloids) have been clinically validated in the treatment of multiple cancers.<sup>1</sup> Eribulin, which is derived from the natural product haricondolyn B, has recently been approved as a microtubule inhibitor with a new mode of action for the treatment of metastatic breast cancer.<sup>2</sup> Microtubules play important roles throughout the cell cycle of cancer cells; however, the disruption of microtubule dynamics produces undesirable side effects, such as neurotoxicity and peripheral neuropathy, which are related to the central role tubulin plays in cell signaling and vesicular transport.<sup>3</sup> Acquired drug resistance is another obstacle that can arise following long-term use of these agents.<sup>4</sup> To overcome these limitations, novel anticancer agents that do not directly act on microtubules are being developed.<sup>5</sup> Kinesin spindle protein (KSP), known as Hs Eg5, a member of the kinesin-5 family, plays an important role in the formation and maintenance of the bipolar spindle.<sup>6</sup> Inhibition of KSP leads to cell cycle arrest during mitosis and results in cells with monopolar spindles (so-called monoasters), followed by apoptosis.<sup>7</sup> As KSP is absent in postmitotic neurons and is likely to act only in dividing cells, its inhibitors might provide better specificity than microtubule inhibitors in the treatment of human malignancies.<sup>8</sup> A large number of KSP inhibitors with various chemical scaffolds have been reported and some of them, including ispinesib (**1**) and filanesib (known as ARRY-520, **2**), have been entered into clinical trials (Figure 1).<sup>9–13</sup> Although the clinical efficacy of these inhibitors has been

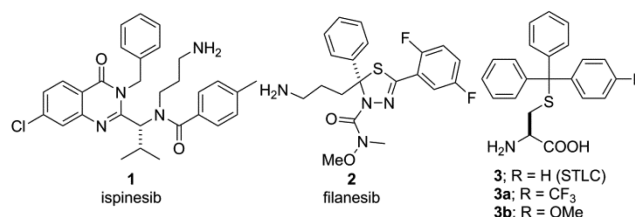


**Figure 1.** Structure of KSP inhibitors: ispinesib (**1**), filanesib (**2**), STLC (**3**), and the previously reported derivatives (**3a** and **3b**).

limited to date, better results have recently been obtained in the treatment of hematological malignancies with thiadiazole-based KSP inhibitors, such as filanesib. Currently, filanesib is undergoing clinical evaluation in combination with proteasome inhibitors such as bortezomib or carfilzomib.<sup>14</sup>

Previously, we reported structure–activity relationship studies (SARs) of S-trityl-L-cysteine (STLC, **3**) derivatives as KSP inhibitors (Figure 1).<sup>15</sup> Several STLC derivatives, such as compounds **3a** and **3b** with a single lipophilic para substituent in one phenyl ring of the trityl group, were 4- to 10-fold more potent than original STLC, in terms of both KSP ATPase inhibition and cell cytotoxicity. Recently, we showed that compound **3a** induces mitotic arrest by activating the mitotic

Received: June 2, 2015

Accepted: July 22, 2015

Published: July 22, 2015

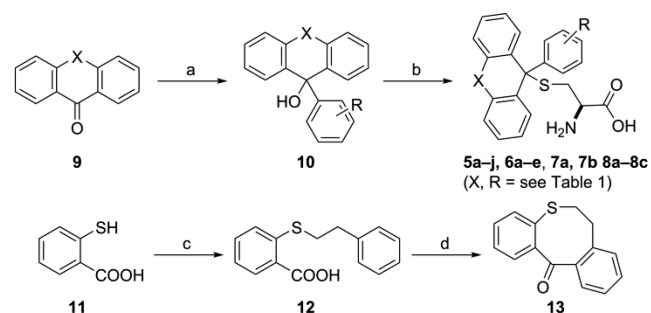
checkpoint, which eventually led to caspase-independent cell death in K562 chronic myeloid cells,<sup>16</sup> as well as demonstrated the capture of KSP in cells by using **3b** immobilized on affinity beads.<sup>17</sup> Kozielski and co-workers, who contributed to the discovery of STLC as a KSP inhibitor,<sup>18,19</sup> have solved the crystal structure of KSP in complex with STLC, revealing that it binds in an allosteric loop L5 binding pocket, as is the case for most other allosteric inhibitors.<sup>20–23</sup> Recently, they reported new STLC-related compounds, where the sulfur atom in STLC was replaced with CH<sub>2</sub>, and the triphenylbutanamine derivatives showed good oral bioavailability and pharmacokinetics.<sup>24,25</sup> According to their data, the trityl group of STLC was situated in a predominantly hydrophobic core region and was involved in hydrophobic interactions. In particular, the aromaticity and configuration of each phenyl ring in the trityl group are important for interactions such as  $\pi$ - $\pi$ , CH- $\pi$ , and edge-to-face interactions with the alkyl side chains of Glu215, Glu116, and Arg119 of KSP, respectively. Based on these findings, we hypothesized that the locking of two phenyl rings with appropriate alkyl chains in the trityl group might afford a configuration that would enable hydrophobic interactions and potent binding to KSP with reduced loss of entropy. Here, we describe a novel series of STLC derivatives with conformationally constrained trityl groups that may contribute to the development of potent KSP inhibitors. We also performed docking simulation of these novel derivatives using AMBER12 and differential scanning fluorimetry (DSF) analysis<sup>26</sup> to investigate the novel ligand–KSP direct interactions. Furthermore, we demonstrated that the representative derivatives **5a–5d** and **6a** significantly suppressed tumor growth in the HCT116 xenograft model.

To confirm our hypothesis, we initially prepared a cross-linked derivative with an ethylene linker between the phenyl rings of the trityl group in STLC and evaluated the inhibitory activity against KSP ATPase. Encouragingly, we found that such a subtle structural variation resulted in compound **4**, which exhibited a 9-fold increase in KSP ATPase inhibition relative to STLC (Figure 2A). To enhance our understanding of why the

inhibition of KSP ATPase was improved by a conformationally constrained compound, we determined a putative binding mode of compound **4** within the well-known allosteric binding pocket of KSP. The possible binding mode of **4** was investigated by a molecular docking experiment via AMBER12 using the previously reported crystal structure of KSP in complex with a *para*-chloro substituted STLC derivative (PDB code: 2xae).<sup>22</sup> Compound **4** was found to dock in an almost completely similar way except for the ethylene linker (Figure 2B). Interestingly, our modeling indicated that the ethylene linker of **4** participates in van der Waals interactions with Tyr211 and Leu214 and CH- $\pi$  interaction with Tyr211, participation that was not seen in the previously reported STLC derivatives. In addition, this binding mode suggested the feasibility of improving the inhibitory activity by introducing a substituent into the nonlinked phenyl ring. We therefore decided to attempt further SARs based on optimization of the cross-linked ring size and the substituent effects of the nonlinked phenyl ring in the trityl group (Figure 2A).

As shown in Scheme 1, target compounds **4**, **5a–j**, **6a–e**, **7a**, **7b**, and **8a–c** were synthesized by the formation of tertiary

### Scheme 1. Synthesis of Novel STLC Derivatives<sup>a</sup>



<sup>a</sup>Reagents and conditions: (a) ArBr, *n*-BuLi, THF, -78 °C, 3 h, then rt, overnight, 70–95%; (b) *L*-cysteine, TFA, rt, 3 h, 15–80%; (c) PhCH<sub>2</sub>CH<sub>2</sub>Br, K<sub>2</sub>CO<sub>3</sub>, acetone, rt to reflux, 3 h, 81%; (d) PPA, 1,4-dioxane, 105 °C, 12 h, then 130 °C, 2 h, 67%.

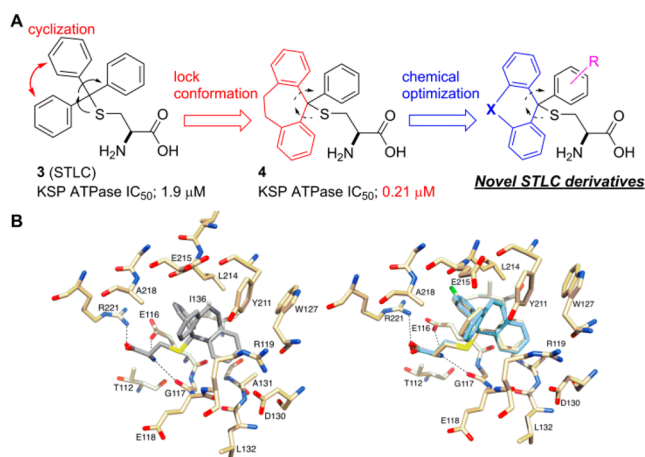


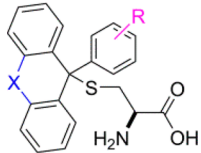
**Figure 2.** Design and docking simulation of novel STLC derivatives. (A) Design of compound **4** and its chemical optimization. (B) Docking mode of compound **4** (left, gray; right, cyan). The protein structure from PDB 2xae was used for docking. The oxygen, nitrogen, and chlorine atoms are colored red, blue, and green, respectively. Hydrogen bonds are shown as dotted lines. The docked pose of compound **4** overlaid with a cocrystal structure of *para*-chloro STLC derivative (right).

alcohols before thioetherification with cysteine in the presence of trifluoroacetic acid, as described previously.<sup>15</sup> Tertiary alcohols were prepared by the reaction of commercially available appropriate ketones with substituted phenyl lithium. The ethylene linker type derivatives, such as compounds **4** and **6c**, were published as glycine transport inhibitors for treating neurological and neuropsychiatric disorders.<sup>27</sup> However, there have been no reports to date of the antitumor activity with the KSP inhibition for those compounds. For the intermediate ketone of compound **8c**, thio-salicylic acid **11** was thio-alkylated by phenethyl bromide and potassium carbonate as a base to give 2-(phenethylthio)benzoic acid **12**, which then underwent intramolecular Friedel–Crafts acylation using polyphosphoric acid to afford the target ketone. As for compounds **7b**, **8b**, and **8c**, which incorporate chiral trityl groups, spectral analysis of the diastereomeric mixtures implied that a 1:1 mixture of the (2*R*, 11*R*) and (2*R*, 11*S*) pairs for **7b** and **8b**, and the (2*R*, 12*R*) and (2*R*, 12*S*) pairs for **8c** had been formed. Attempts to separate these using HPLC proved unsuccessful, so we prepared and assayed them as diastereomeric mixtures. Comparisons between compounds should therefore be viewed from a SAR perspective as relative. The synthetic processes and

physical data for the intermediate and final compounds are reported in the [Supporting Information](#).

The newly synthesized compounds were evaluated for KSP ATPase inhibition and cytotoxicity toward HCT116 cells, together with the previously reported compounds (**3**, **3a**, and **3b**) as controls and the clinical candidate benchmarks (**1** and **2**) ([Table 1](#)). We first investigated the substituent effects on the

**Table 1. Inhibitory Activity on KSP ATPase and HCT-116 Cell Proliferation**



| compd                   | X                                   | R                 | KSP ATPase<br>IC <sub>50</sub> <sup>a</sup> (nM) | cytotoxicity <sup>b</sup><br>IC <sub>50</sub> <sup>a</sup> (nM) |
|-------------------------|-------------------------------------|-------------------|--|---|
| <b>3</b> (STLC)         |                                     | H                 | 1900 ± 230                                       | 910 ± 58  |
| <b>3a</b>               |                                     | 4-CF <sub>3</sub> | 262 ± 17   | 216 ± 14  |
| <b>3b</b>               |                                     | 4-OMe             | 166 ± 8.8  | 213 ± 4.4   |
| <b>4</b>                | -CH <sub>2</sub> CH <sub>2</sub> -  |                   | 209 ± 34   | 325 ± 15  |
| <b>5a</b>               | -CH <sub>2</sub> CH <sub>2</sub> -  | 4-CF <sub>3</sub> | 21 ± 1.7   | 11 ± 0.6  |
| <b>5b</b>               | -CH <sub>2</sub> CH <sub>2</sub> -  | 4-OMe             | 14 ± 1.2   | 28 ± 1.1  |
| <b>5c</b>               | -CH <sub>2</sub> CH <sub>2</sub> -  | 4-Me              | 9.3 ± 0.2  | 25 ± 1.1  |
| <b>5d</b>               | -CH <sub>2</sub> CH <sub>2</sub> -  | 4-Cl              | 11 ± 1.3   | 41 ± 0.6  |
| <b>5e</b>               | -CH <sub>2</sub> CH <sub>2</sub> -  | 4-Ph              | 1060 ± 120                                       | 1300 ± 54   |
| <b>5f</b>               | -CH <sub>2</sub> CH <sub>2</sub> -  | 4-PhO             | 306 ± 13   | 291 ± 6.3   |
| <b>5g</b>               | -CH <sub>2</sub> CH <sub>2</sub> -  | 4- <i>t</i> Bu    | 301 ± 13   | 234 ± 13  |
| <b>5h</b>               | -CH <sub>2</sub> CH <sub>2</sub> -  | 3-CF <sub>3</sub> | 238 ± 38   | 123 ± 7.0   |
| <b>5i</b>               | -CH <sub>2</sub> CH <sub>2</sub> -  | 3-Cl              | 160 ± 45   | 637 ± 33  |
| <b>5j</b>               | -CH <sub>2</sub> CH <sub>2</sub> -  | 2-Me              | 7800 ± 550                                       | 4590 ± 270  |
| <b>6a</b>               | -CH=CH-                             | 4-CF <sub>3</sub> | 36 ± 0.7   | 5.0 ± 0.3   |
| <b>6b</b>               | -CH=CH-                             | 4-OMe             | 8.6 ± 1.1  | 2.6 ± 0.4   |
| <b>6c</b>               | -CH=CH-                             | 4-Me              | 14 ± 1.6   | 3.4 ± 0.1   |
| <b>6d</b>               | -CH=CH-                             | 4-Cl              | 12 ± 1.7   | 3.9 ± 0.1   |
| <b>6e</b>               | -CH=CH-                             | 4-Ph              | 1400 ± 300                                       | 395 ± 4.7   |
| <b>7a</b>               | -O-                                 | 4-CF <sub>3</sub> | >20000   | >10000  |
| <b>7b</b>               | -CH <sub>2</sub> O-                 | 4-CF <sub>3</sub> | 75 ± 4.7   | 76 ± 2.4  |
| <b>8a</b>               | -S-                                 | 4-CF <sub>3</sub> | >20000   | >10000  |
| <b>8b</b>               | -CH <sub>2</sub> S-                 | 4-CF <sub>3</sub> | 61 ± 8.7   | 15 ± 0.9  |
| <b>8c</b>               | -CH <sub>2</sub> CH <sub>2</sub> S- | 4-CF <sub>3</sub> | >20000   | >10000  |
| <b>1</b><br>(ispinesib) |                                     |                   | 47 ± 0.6   | 1.1 ± 0.1   |
| <b>2</b> (filanesib)    |                                     |                   | 18 ± 0.4   | 0.7 ± 0.1   |

<sup>a</sup>IC<sub>50</sub> values are shown as means ± SEM (for potent compounds only) from at least three independent dose–response curves. <sup>b</sup>HCT116 cells.

nonlinked phenyl ring in compound **4**. Most encouragingly, compared with **4**, the introduction of a 4-trifluoromethyl moiety afforded compound **5a**, which showed a 10-fold increase in KSP ATPase inhibition and a 30-fold increase in cytotoxic activity, while a 4-methoxy moiety afforded compound **5b** giving a 15-fold increase in KSP ATPase inhibition and a 12-fold increase in cytotoxic activity. Furthermore, compounds **5c** (4-Me) and **5d** (4-Cl), with similar size substituents as compounds **5a** and **5b**, also displayed excellent KSP ATPase inhibition and potent cytotoxicity. Compared with **3**, compounds **5a–5d** exhibited double-digit increases in KSP ATPase inhibition and 22- to 83-fold increases in inhibitory

activity against HCT116 cells. Although cytotoxicity of compounds **5a–5d** were less potent than that of **1** and **2**, KSP ATPase inhibitory activity of those were comparable. We then investigated the size and substitution position of the substituents in **4**. Incorporation of a 4-phenyl substituent (**5e**) resulted in loss of potency, while derivatives with similar bulky substituents (4-PhO, **5f**; 4-*t*Bu, **5g**) were equipotent with **4**. Regarding the positions of the substituents, derivatives with 3-CF<sub>3</sub> (**5h**) and 3-Cl (**5i**) were better tolerated compared with **4** but were more than 10 times weaker than the corresponding 4-substituent derivatives. In addition, 2-Me (**5j**) was more than 10 times weaker than **4**. These results suggest that a small lipophilic substituent at the para position is essential for a high level of KSP ATPase inhibition and cytotoxic activities, as reported in our previous SARs of STLC derivatives.<sup>15</sup>

Next, we investigated the modification of the cross-linked alkyl chain and the ring size. Among derivatives **6a–6d**, which have the same substituents as compounds **5a–5d**, respectively, replacement of the C–C single bond with a C=C double bond also afforded potent inhibitory activity against KSP ATPase. It should be noted that compounds **6a–6e** showed more potent cytotoxic activity than the corresponding derivatives **5a–5e**, except for **6e**, with inhibitory activity in the single-digit nanomolar range. Although the reasons for this enhanced cytotoxicity were not obvious, the cytotoxicity of these derivatives presumably reflected different levels of cell permeability because the ClogP value of a compound with a double bond tends to be higher than that of a single bond.<sup>28</sup> Replacement of the C–C bond with C–O (**7b**) and C–S (**8b**) bonds slightly reduced the KSP ATPase inhibitory activity but retained the cell cytotoxicity compared with the corresponding substituent of **5a**. Interestingly, changing the linked ring size in compound **5a** led to a dramatic loss of potency. Replacement of the two carbons with O (**7a**), S (**8a**), and CH<sub>2</sub>–CH<sub>2</sub>–S (**8c**) resulted in substantial loss of potency. These SARs indicate that appropriate restriction of the rotatable phenyl ring in the trityl group has favorable effects on the inhibition of KSP ATPase and cytotoxic activities. Thus, an optimal size for the linked ring, which has a cross-linked alkyl chain length of two atoms and a single lipophilic para substituent in the nonlinked phenyl ring of the trityl group, is an essential requirement for the potent inhibition of KSP by the new STLC derivatives.

We next performed DSF analysis<sup>26</sup> to investigate the direct interactions between the novel ring-linked STLC derivatives with KSP. The ability to stabilize KSP was assessed by measuring the thermal stability of the KSP native protein and the protein complex with the ligand. Complexes of each compound were heated stepwise in the presence of the fluorescent dye whose fluorescence increases when it interacts with the hydrophobic residues of the protein. These residues become exposed to the dye when the protein is denatured. A higher positive shift of *T*<sub>m</sub> in comparison to complexes with an inactive compound, such as dibenzyl-*L*-cysteine ( $\Delta T_m$  0.0 °C, KSP ATPase IC<sub>50</sub> > 63.0 μM), means greater stabilization of the complexes, which is a consequence of a direct inhibitor binding. The positive control experiment using **3** as a ligand confirmed a significant improvement in the stability of the complex ( $\Delta T_m$  5.0 °C) in the presence of nucleotide as reported previously.<sup>29</sup> Furthermore, as expected, the degree of rise in the *T*<sub>m</sub> shift value correlated with the potency of KSP inhibitory activity in the compound series (**4**,  $\Delta T_m$  8.0 °C; **3b**,  $\Delta T_m$  9.0 °C; **5b**,  $\Delta T_m$  12.0 °C; **6b**,  $\Delta T_m$  12.5 °C; [Figure 3A](#)). These results suggest that STLC derivatives in this series

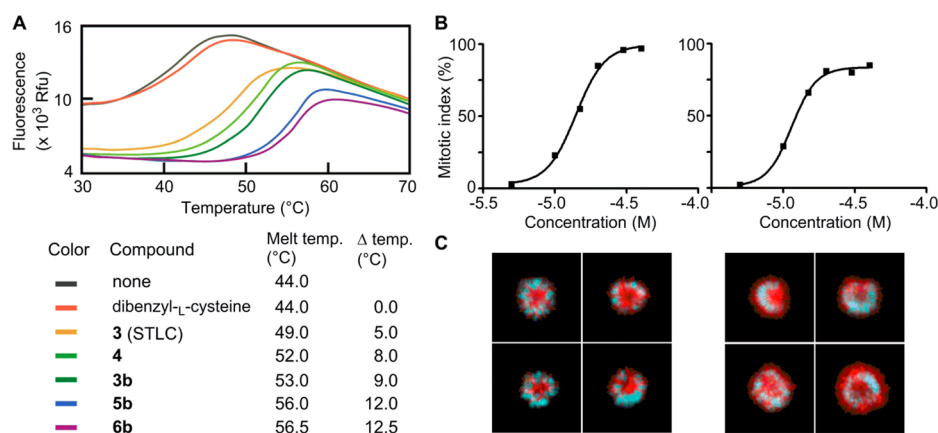


**Figure 3.** Affinity of the STLC derivatives to KSP motor domain and effect on cell proliferation. (A) Compounds interacted with and thermal-stabilized KSP motor domain in the presence of ATP. The fluorescence profiles of Sypro Orange obtained using  $4 \mu\text{M}$  of the KSP motor domain in the presence of various compounds at  $100 \mu\text{M}$  along with  $1 \text{ mM}$  of ATP by differential scanning fluorimetry. The gray line indicates that no inhibitor was added. The color of each line indicates the individual compound used. The melting temperatures of the KSP motor domain in the absence and presence of compounds were presented. The compound-mediated thermal shifts were also shown as  $\Delta$ temperatures. (B,C) Effect of **5a** (left) and **6a** (right) on cell proliferation. Mitotic index dose–response curve (B) and mitotic phenotype (C) of HeLa cells treated with compound **5a** ( $40 \text{ nM}$ ) and compound **6a** ( $40 \text{ nM}$ ). Chromosomes are colored blue and the microtubules red.

directly bind to KSP and that the inhibitory activity depends on the potency of the KSP–ligand binding affinity.

We previously demonstrated that **3a** and **3b** did not inhibit ATPase activity of other kinesins such as centromere-associated protein E (CENP-E), kid, KIF4, and mitotic kinesin-like protein 1 (MKLP-1).<sup>15</sup> The ATPase inhibitory activities of newly synthesized derivatives such as **5a** and **5b** were evaluated for those motor proteins. Neither those kinesins nor additionally evaluated kinesins such as KIF15 and KIF3C were inhibited by **5a** or **5b** (Supporting Information Figure S1). Furthermore, an excellent positive correlation between KSP ATPase inhibition and cell cytotoxicity was observed (Table 1 and Supporting Information Figure S2). We then investigated the effects on cell cycle progression. The  $\text{MI}_{50}$  values (50% mitotic index induction concentration) of compounds **5a** and **6a** were correlated with that of the level of cytotoxicity (**5a**,  $\text{MI}_{50}$   $14 \text{ nM}$ ; **6a**,  $\text{MI}_{50}$   $12 \text{ nM}$ ) (Figure 3B). Microscopic analysis of the mitotic phenotype of the cells treated with **5a** or **6a** showed the formation of monopolar spindles, the typical phenotype of KSP inhibition, in all cells during mitotic arrest (Figure 3C). Taken together, we demonstrate that the newly designed derivatives with two fused phenyl rings in the trityl group inhibit KSP in cells and the inhibition of KSP subsequently induced M-phase arrest with typical monoastal phenotype.

The in vivo antitumor effects of the representative compounds were examined in the HCT116 xenograft model (Table 2 and Supporting Information Figure S3). To improve the solubility of these candidates, a sodium salt of each compound was prepared with no differences observed in in vitro activities (Supporting Information Table S1). Treatment mice received compounds as intravenous injections on days 1, 3, 5, 8, 10, and 12. Compounds **4**, **5a**, and **6a** demonstrated dose-dependent antitumor activity in this model. At a dose of  $150 \text{ mg/kg}$ , compound **4** inhibited tumor growth (T/C: 23%). At a  $75 \text{ mg/kg}$  dose, compound **4** showed moderate inhibition of tumor growth (T/C: 43%). At the same dose, compound **5a**, which exhibited approximately a 30-fold increase in cytotoxicity against HCT116 cells compared with **4**, was more potent (T/C: 9%). Whereas compound **4** showed weak inhibition of tumor growth (T/C: 62%) at a dose of  $25 \text{ mg/kg}$ , compounds

**Table 2.** Antitumor Activity in the HCT116 Xenograft Model upon Treatment with Newly Synthesized Derivatives

| compd     | dose (mg/kg) | T/C (%) <sup>a</sup> | mortality |
|-----------|--------------|----------------------|-----------|
| <b>4</b>  | 150          | 23 <sup>c</sup>      | 0/6       |
| <b>4</b>  | 75           | 43 <sup>b</sup>      | 0/6       |
| <b>4</b>  | 25           | 62 <sup>b</sup>      | 0/6       |
| <b>5a</b> | 75           | 9 <sup>c</sup>       | 0/6       |
| <b>5a</b> | 25           | 21 <sup>c</sup>      | 0/6       |
| <b>5b</b> | 25           | 26 <sup>c</sup>      | 0/6       |
| <b>5c</b> | 25           | 19 <sup>c</sup>      | 0/6       |
| <b>5d</b> | 25           | 11 <sup>c</sup>      | 0/6       |
| <b>6a</b> | 25           | 12 <sup>c</sup>      | 0/6       |
| <b>6a</b> | 10           | 31 <sup>b</sup>      | 0/6       |

<sup>a</sup>T/C (%) = (mean tumor weight of treated group)/(mean tumor weight of control group)  $\times 100$ ,  $n = 6$ . <sup>b</sup> $p < 0.0001$ . <sup>c</sup> $p < 0.00001$  vs control.

**5a–5d** and **6a** showed significant suppression of HCT-116 cell growth ( $P < 0.00001$ ) on day 15. With regard to body weight change by the compound treatment, slight to moderate body weight loss was observed against the vehicle control (Supporting Information Figure S3). To assess the exact efficacy and toxicity of those compounds, it is necessary to optimize the amount, schedule, and route of administration. However, none of the mice died during the treatment under the condition used in this study. These pharmacological studies with HCT-116 xenograft models demonstrated the potent antitumor efficacy of the STLC derivatives with locked phenyl rings. The most potent group of the derivatives such as compounds **5a–5d** and **6a** in the in vitro studies also exhibited potent antitumor activity in vivo, suggesting that the antitumor activity of those derivatives depend on the KSP inhibition in the tumor. Although the details for the effect of those derivatives on tumor microenvironment still remained to be elucidated, the newly identified STLC derivatives could be potent lead compounds for developing next-generation KSP inhibitors and probing biological function of KSP in tumor microenvironment.

In summary, a series of novel STLC derivatives were designed by a structure-guided approach, and those were

synthesized and biologically evaluated as KSP inhibitors. The SARs data indicate that the two linked phenyl rings and the nonlinked phenyl ring with a small lipophilic para substituent in the trityl group enabled better binding by occupying a hydrophobic pocket in the STLC binding site. The modeling results indicated that van der Waals interactions between the new STLC derivatives and KSP might contribute to the improvements seen in inhibitory activities. New derivatives, such as **5a–5d** and **6a–6d**, displayed potent KSP ATPase inhibition and cell cytotoxicity in the nanomolar range. In addition, excellent correlation was observed between the inhibitory activities. DSF analysis showed direct binding of the STLC derivatives and KSP and revealed that inhibitory activity was dependent on the potency of the binding affinity to the protein. Representative compounds **5a** and **6a** arrested cells in mitosis, leading to formation of the monopolar spindle phenotype. Furthermore, compounds **5a–5d** and **6a** significantly suppressed HCT116 xenograft tumor growth in vivo. Thus, the STLC derivatives with two linked phenyl rings could be novel lead compounds in the design of clinical candidates for next-generation KSP inhibitors as antitumor chemotherapies. Although limited clinical responses have been reported for almost all KSP inhibitors examined as monotherapies, the use of KSP inhibitors, such as **2**, in combination with other anticancer drugs to improve the clinical effects is still an attractive prospect. Further detailed studies of this novel STLC series, including X-ray cocrystallization, in vivo evaluation, and the exploration of predictive biomarkers, are in progress.

## ■ ASSOCIATED CONTENT

### Supporting Information

The Supporting Information is available free of charge on the ACS Publications website at DOI: [10.1021/acsmchemlett.5b00221](https://doi.org/10.1021/acsmchemlett.5b00221).

Figures, table, compound characterization, and methods for syntheses and biological studies (PDF)

## ■ AUTHOR INFORMATION

### Corresponding Author

\*Phone: +81-54-264-5231. Fax: +81-54-264-5231. E-mail: [aasai@u-shizuoka-ken.ac.jp](mailto:aasai@u-shizuoka-ken.ac.jp).

### Present Address

<sup>||</sup>Department of Chemistry and Life Science School of Advanced Engineering, Kogakuin University, Tokyo, 192–0015, Japan.

### Funding

This work was supported by the Drug Discovery Program of the Pharma Valley Center and JSPS KAKENHI Grant Number 26460150.

### Notes

The authors declare no competing financial interest.

## ■ ACKNOWLEDGMENTS

The authors thank Ms. Chika Tokuyama for excellent technical assistance in biological evaluations.

## ■ ABBREVIATIONS

KSP, kinesin spindle protein; STLC, S-trityl-L-cysteine; TFA, trifluoroacetic acid; PPA, polyphosphoric acid; DSF, differential scanning fluorimetry; CENP-E, centromere-associated protein E; MKLP-1, mitotic kinesin-like protein 1

## ■ REFERENCES

- (1) Dutcher, J. P.; Novik, Y.; O'Boyle, K.; Marcoullis, G.; Secco, C.; Wiernik, P. H. 20th-century advances in drug therapy in oncology -part II. *J. Clin. Pharmacol.* **2000**, *40*, 1079–1092.
- (2) Jain, S.; Vahdat, L. T. Eribulin Mesylate. *Clin. Cancer Res.* **2011**, *17*, 6615–6622.
- (3) Jordan, M. A.; Wilson, L. Microtubules as a target for anticancer drugs. *Nat. Rev. Cancer* **2004**, *4*, 253–265.
- (4) Kavallaris, M. Microtubules and resistance to tubulin binding agents. *Nat. Rev. Cancer* **2010**, *10*, 194–204.
- (5) Jackson, K. W.; Patrick, D. R.; Dar, M. M.; Huang, P. S. Targeted anti-mitotic therapies: can we improve on tubulin agents? *Nat. Rev. Cancer* **2007**, *7*, 107–117.
- (6) Slangy, A.; Lane, H. A.; d'Herin, P.; Harper, M.; Kress, M.; Nigg, E. A. Phosphorylation by p34cdc2 regulates spindle association of human Eg5, a kinesin-related motor essential for bipolar spindle formation in vivo. *Cell* **1995**, *83*, 1159–1169.
- (7) Mayer, T. U.; Kapoor, T. M.; Haggarty, S. J.; King, R. W.; Schreiber, S. L.; Mitchison, T. L. Small molecule inhibitor of mitotic spindle bipolarity identified in a phenotype-based screen. *Science* **1999**, *286*, 971–974.
- (8) Sarli, V.; Giannis, A. Targeting the kinesin spindle protein: basic principles and clinical implications. *Clin. Cancer Res.* **2008**, *14*, 7583–7587.
- (9) Rath, O.; Kozielski, F. Kinesins and cancers. *Nat. Rev. Cancer* **2012**, *12*, 527–539.
- (10) El-Nassan, H. B. Advances in the discovery of kinesin spindle protein (Eg5) inhibitors as antitumor agents. *Eur. J. Med. Chem.* **2013**, *62*, 614–631.
- (11) Burris, H. A., III; Jones, S. F.; Williams, D. D.; Kathman, S. J.; Hodge, J. P.; Pandite, L.; Ho, P. T.; Boerner, S. A.; Lorusso, P. A phase I study of ipinesib, a kinesin spindle protein inhibitor, administered weekly for three consecutive weeks of a 28-day cycle in patients with solid tumors. *Invest. New Drugs* **2011**, *29*, 467–472.
- (12) Woessner, R.; Tunquist, B.; Lemieux, C.; Chlipala, E.; Jackinsky, S.; Dewolf, W.; Voegtli, W.; Cox, A.; Rana, S.; Lee, P.; Walker, D. ARRY-520, a novel KSP inhibitor with potent activity in hematological and taxane-resistant tumor models. *Anticancer Res.* **2009**, *29*, 4373–4380.
- (13) Khoury, H. J.; Garcia-Manero, G.; Borthakur, G.; Kadia, T.; Foudray, M. C.; Arellano, M.; Langston, A.; Bethelme-Bryan, B.; Rush, S.; Litwiler, K.; Karan, S.; Simmons, H.; Marcus, A. I.; Ptaszynski, M.; Kantarjian, H. A phase I dose-escalation study of ARRY-520, a kinesin spindle protein inhibitor, in patients with advanced myeloid leukemias. *Cancer* **2012**, *14*, 3556–3564.
- (14) Ocio, E. M.; Mitsiades, C. S.; Orłowski, R. Z. Future agents and treatment directions in multiple myeloma. *Expert Rev. Hematol.* **2014**, *7*, 127–141.
- (15) Ogo, N.; Oishi, S.; Matsuno, K.; Sawada, J.-i.; Fujii, N.; Asai, A. Synthesis and biological evaluation of L-cysteine derivatives as mitotic kinesin Eg5 inhibitors. *Bioorg. Med. Chem. Lett.* **2007**, *17*, 3921–3924.
- (16) Shimizu, M.; Ishii, H.; Ogo, N.; Unno, Y.; Matsuno, K.; Sawada, J.-i.; Akiyama, Y.; Asai, A. S-trityl-L-cysteine derivative induces caspase-independent cell death in K562 human chronic myeloid cell line. *Cancer Lett.* **2010**, *298*, 99–106.
- (17) Shimizu, M.; Ishii, H.; Ogo, N.; Matsuno, K.; Asai, A. Biochemical analysis of cellular target of S-trityl-L-cysteine derivatives using affinity matrix. *Bioorg. Med. Chem. Lett.* **2010**, *20*, 1578–1580.
- (18) Debonis, S.; Skoufias, D. A.; Lebeau, L.; Lopez, R.; Robin, G.; Margolis, R. L.; Wade, R. H.; Kozielski, F. In vitro screening for inhibitors of the human mitotic kinesin Eg5 with antimitotic and antitumor activities. *Mol. Cancer Ther.* **2004**, *3*, 1079–1090.
- (19) Skoufias, D. A.; Debonis, S.; Saoudi, Y.; Lebeau, L.; Crevel, I.; Cross, R.; Wade, R. H.; Hackney, D.; Kozielski, F. S-trityl-L-cysteine is a reversible, tight binding inhibitor of the human kinesin Eg5 that specifically blocks mitotic progression. *J. Biol. Chem.* **2006**, *281*, 17559–17569.

(20) Kaan, H. Y. K.; Ulaganathan, V.; Hackney, D. D.; Kozielski, F. An allosteric transition trapped in an intermediate state of a new kinesin-inhibitor complex. *Biochem. J.* **2010**, *425*, 55–60.

(21) Debonis, S.; Skoufias, D. A.; Indorato, R.-L.; Liger, F.; Marquet, B.; Laggner, B.; Kozielski, F. Structure-activity relationship of *S*-trityl-L-cysteine analogues as inhibitors of the human mitotic kinesin Eg5. *J. Med. Chem.* **2008**, *51*, 1115–1125.

(22) Kaan, H. Y. K.; Weiss, J.; Menger, D.; Ulaganathan, V.; Tkocz, K.; Laggner, C.; popowycz, F.; Joseph, B.; Kozielski, F. Structure-activity relationship and multigrug resistance study of new of *S*-trityl-L-cysteine derivatives as inhibitors of Eg5. *J. Med. Chem.* **2011**, *54*, 1576–1586.

(23) Abualhasan, M. N.; Good, J. A.; Wittayanarakul, K.; Anthony, N. G.; Berretta, G.; Rath, O.; Kozielski, F.; Sutcliffe, O. B.; Mackay, S. P. Doing the methylene shuffle—further insights into the inhibition of mitotic kinesin Eg5 with *S*-trityl-L-cysteine. *Eur. J. Med. Chem.* **2012**, *54*, 483–498.

(24) Wang, F.; Good, J. A. D.; Rath, O.; Kaan, H. Y. K.; Sutcliffe, O. B.; Mackay, S. P.; Kozielski, F. Triphenylbutanamines: kinesin spindle protein inhibitors with in vivo antitumor activity. *J. Med. Chem.* **2012**, *55*, 1511–1525.

(25) Good, J. A. D.; Wang, F.; Rath, O.; Kaan, H. Y. K.; Talapatra, S. K.; Podgorski, D.; Mackay, S. P.; Kozielski, F. Optimization *S*-trityl-L-cysteine-based inhibitors of kinesin spindle protein with potent in vivo antitumor activity in lung cancer xenograft models. *J. Med. Chem.* **2013**, *56*, 1878–1893.

(26) Niesen, F. H.; Berglund, H.; Vedadi, M. The use of differential scanning fluorimetry to detect ligand interactions that promote protein stability. *Nat. Protoc.* **2007**, *2*, 2212–2221.

(27) Ognyanov, V. I.; Bell, S. C.; Hopper, A.; Zhang, J. Tricyclic compounds as glycine transport inhibitors. WO9941227A1, Aug 19, 1999.

(28) The ClogP values of compounds **6a–6d** were 4.65, 3.69, 4.27, and 4.48, whereas ClogP values of compounds **5a–5d** were 4.41, 3.44, 4.02, and 4.24, respectively. The ClogP values were calculated by ChemBioDraw Ultra 14.0.

(29) Yokoyama, H.; Sawada, J.-i.; Katoh, S.; Matsuno, K.; Ogo, N.; Ishikawa, Y.; Hashimoto, H.; Fujii, S.; Asai, A. Structural basis of new allosteric inhibition in kinesin spindle protein Eg5. *ACS Chem. Biol.* **2015**, *10*, 1128–1136.